AGU PUBLICATIONS

JGR

Journal of Geophysical Research: Atmospheres

RESEARCH ARTICLE

10.1002/2015JD024447

Key Points:
- Idealized stratospheric model accurately simulates CMAM trace gas and mean age profiles
- Idealized model provides quantitative transport guidance for CCM to better simulate observations
- Specific suite of trace gas measurements provides unique transport information to validate CCMs

Correspondence to:
E. A. Ray,
eric.ray@noaa.gov

Citation:
Ray, E. A., F. L. Moore, K. H. Rosenlof, D. A. Plummer, F. Kolonjari, and K. A. Walker (2016), An idealized stratospheric model useful for understanding differences between long-lived trace gas measurements and global chemistry-climate model output, *J. Geophys. Res. Atmos.*, *121*, 5356–5367, doi:10.1002/2015JD024447.

Received 3 NOV 2015
Accepted 1 MAY 2016
Accepted article online 5 MAY 2016
Published online 19 MAY 2016

An idealized stratospheric model useful for understanding differences between long-lived trace gas measurements and global chemistry-climate model output

Eric A. Ray[1,3], Fred L. Moore[2,3], Karen H. Rosenlof[1], David A. Plummer[4], Felicia Kolonjari[5], and Kaley A. Walker[5]

[1]Chemical Sciences Division, NOAA Earth System Research Laboratory, BoulderColorado, USA, [2]Global Monitoring Division, NOAA Earth System Research Laboratory, Boulder, Colorado, USA, [3]Cooperative Institute for Research in Environmental Sciences, University of Colorado Boulder, Boulder, Colorado, USA, [4]Canadian Centre for Climate Modeling and Analysis, Environment Canada, Montreal, Quebec, Canada, [5]Department of Physics, University of Toronto, Toronto, Ontario, Canada

Abstract We use a modified version of the tropical leaky pipe (TLP) model of the stratosphere to explore how well an idealized model can (1) reproduce global chemistry-climate model (CCM) output and (2) constrain transport characteristics necessary to replicate measurements of long-lived trace gases. The version of the TLP model we use includes the simulation of long-lived trace gases, such as SF_6 and CO_2, as well as photochemically active trace gases such as CFC-11, CFC-12, and N_2O. The TLP model was found to accurately replicate trace gas output from the Canadian Middle Atmosphere Model (CMAM) for time-averaged profiles in the tropics and each extratropical region. Given confidence that the TLP model represents the basic transport features in CMAM we then used the TLP model to interpret differences between CMAM output and measurements from the Atmospheric Chemistry Experiment and balloons. The TLP model is shown to uniquely determine residual mean circulation and recirculation (mixing between the extratropics and tropics) changes necessary for CMAM to more accurately simulate the measurements. Such guidance on these transport parameters is novel due to the relatively high precision and the simultaneous derivation of important parameters, as compared to previous studies. The TLP model can ideally be used as a bridge between measurements and CCMs to potentially allow more targeted modification of the CCMs than would otherwise be possible.

1. Introduction

The stratosphere is increasingly being recognized as an important component in understanding the climate system and how it is changing [e.g., *Gerber et al.*, 2012; *Kidston et al.*, 2015]. Chemistry climate models (CCMs) now consistently incorporate high tops that encompass the stratosphere and even mesosphere but there is still a significant amount of spread in many aspects of the stratospheric simulations [e.g., *Manzini et al.*, 2014]. CCMs also have persistent biases in the simulation of the stratosphere when compared to available observations [*Butchart et al.*, 2011].

The stratosphere is characterized by relatively rapid horizontal transport (on the order of days) over large latitudinal regions by Rossby waves [*McIntyre and Palmer*, 1983], compared to slow vertical transport of months per kilometer [*Rosenlof*, 1995]. By contrast, in the troposphere, the vertical transport in convective updrafts can take less than an hour to cover 15 km [*Bertram et al.*, 2007]. The characteristics of the stratospheric transport of air have two important implications. The first is that regions of the stratosphere not separated by a mixing “barrier” can be well mixed, such that individual measurements within that region can often be representative of the whole region [e.g., *Plumb*, 1996]. The second is that slow vertical motion means that air parcels remain in the stratosphere for many years, some for more than a decade [e.g., *Waugh and Hall*, 2002; *Li et al.*, 2012]. The amount of time an air parcel has spent in the stratosphere is referred to as the stratospheric age of air. Each air parcel is composed of particles with a range of ages that can be characterized by the width of the age of air distribution. This age distribution implies that it is necessary to accurately simulate the stratospheric circulation for periods of several years or more, depending on the location, prior to the time of an observation of a long-lived trace gas to accurately simulate the trace gas mixing ratio.

The Tropical Pipe (TP) idealized model of the stratosphere was designed to take advantage of the horizontally well-mixed aspect of the stratosphere by reducing the model horizontal dimension to three 1-D regions, the zonally averaged tropics, and each of the northern and southern extratropics [*Plumb*, 1996]. The TP model was subsequently modified to allow mixing between the extratropics and tropics, to better match observed trace gas distributions [*Neu and Plumb*, 1999]. This Tropical "Leaky" Pipe (TLP) model has since been used in a number of studies, primarily in the examination of the mean age of stratospheric air [e.g., *Hall and Waugh*, 2000] but also in the analysis of trace gas distributions [e.g., *Stolarski et al*., 2014]. The TLP model in these studies was successful in simulating aspects of stratospheric trace gases and mean age under steady state conditions. But the stratospheric circulation is not in steady state and instead has significant variability on time scales from seasonal to decadal [e.g., *Ray et al*., 2014]. All of these time scales of variability imprint on the distribution of trace gases in the stratosphere so it is necessary to include them to make an accurate simulation at any particular time.

In *Ray et al*. [2010] the TLP model was used to simulate transient responses of the stratospheric tropical and northern hemispheric average mean age and ozone distributions to volcanic, sea surface temperature-related, and long-term perturbations to the stratospheric circulation. This extension of the TLP model to include temporal variability and a trace gas with photochemical sources and sinks began to show how the model could elucidate cause and effect between specific stratospheric transport features and measured or modeled trace gas distributions. In *Moore et al*. [2014] the TLP model was modified to include a range of photochemical trace gases and age of air in order to demonstrate the sampling frequency of a potential measurement program. Subsequently, in *Ray et al*. [2014], the TLP model was further modified to include detailed aspects of the stratospheric mean circulation and mixing over the past four decades to help better understand balloon-based in situ trace gas measurements over that time period [*Engel et al*., 2009]. This version of the model included forward particle trajectories released at each time step, full photochemistry for photolytic trace gases and time varying input for tracers in growth. The output from the model was able to accurately simulate the observations and contains detailed aspects of mean age temporal variability seen in global CCMs. This work also indicated that mean age based on trace gas measurements alone cannot constrain both the stratospheric mean circulation and mixing. As discussed in *Moore et al*. [2014] and shown in this work, a combination of photochemical trace gases and mean age is necessary to fully constrain both the stratospheric mean circulation and mixing.

A number of previous studies have used trace gas distributions to derive aspects of the stratospheric transport. The imprint of tropical tropopause temperatures on the stratospheric water vapor mixing ratios has been used to derive tropical upwelling rates and rates of mixing from the extratropics into the tropics [e.g., *Mote et al*., 1998; *Schoeberl et al*., 2008]. The combination of multiple trace gases with unique sensitivities has been shown to be particularly useful for constraining stratospheric transport quantities [e.g., *Volk et al*., 1996; *Minschwaner et al*., 1996; *Hall*, 2000; *Schoeberl et al*., 2005; *Strahan et al*., 2011]. In this study we build on this previous work using the specific combination of mean age and the photolytic trace gases, CFC-11 and CFC-12. Each of these trace gases has a unique sensitivity to the mean circulation and mixing in different regions of the stratosphere. The TLP model is capable of quantifying these transport parameters based on the mean age and photolytic trace gas combination with higher precision and less uncertainty compared to previous studies and includes seasonal, quasi-biennial oscillation (QBO), and other interannual variability.

The main advantage of an idealized model is that it can be used to explore a range of possibilities that would be difficult or costly to do with multiple comprehensive global model scenarios. In the case of the idealized TLP model, a range of stratospheric mean circulation and mixing possibilities can be easily explored. The mean circulation and mixing have direct impacts on stratospheric trace gas distributions, thus can be directly compared to observations. In a global CCM the stratospheric mean circulation and mixing are determined by details of the propagation of waves into the stratosphere from a variety of tropospheric sources [e.g., *McLandress and Shepherd*, 2009]. This means that how faithfully CCM output compares to stratospheric observations is primarily dependent on how well the model simulates tropospheric wave activity and some aspects of the stratospheric zonal winds. There are many factors that determine the strength and distribution of tropospheric wave activity. Testing modification of these factors to assess impacts on the mean circulation and mixing that result in better simulations of trace gas distributions is costly and time-consuming. The TLP model can potentially act as an intermediary to test aspects of the stratospheric transport that directly impact observations. Ideally, with this guidance a global CCM could better target specific combinations of the stratospheric residual mean circulation and mixing indicated by the TLP model to best reproduce the observations.

In this paper we describe the modified TLP model used in *Ray et al*. [2014], and new results from simulations of the modified TLP model done to identify why the output from the Canadian Middle Atmosphere Model (CMAM) guided by ERA-Interim reanalysis does not accurately reproduce stratospheric trace gas measurements from the Atmospheric Chemistry Experiment (ACE). The goals are to demonstrate first that the TLP model can reproduce average output from a global CCM and, second, can be used to determine how the large-scale stratospheric transport in the global CCM needs to change to match the measurements.

2. Global CCM Output and Satellite Measurements

In this work we use output from the Canadian Middle Atmosphere Model (CMAM) [*Scinocca et al*., 2008]. The CMAM is a state-of-the-art CCM that has been shown to reproduce many aspects of the chemical and dynamical climate of the stratosphere [*Stratospheric Processes and their Role in Climate Chemistry-Climate Model Validation Activity (SPARC CCMVal)*, 2010]. For the specific runs used here the model was run at T47 horizontal spectral resolution (approximately 3.8°) with 71 vertical levels from the surface to approximately 95 km altitude. Additionally, the CMAM was run in "specified dynamics" mode, whereby the dynamical fields (winds and temperature) of CMAM were "nudged" toward the ERA-Interim [*Dee et al*., 2011] reanalysis. The nudging consists of applying an additional tendency to the model horizontal winds and temperature designed to relax the difference between the model and the reanalysis with a time constant of 24 h and is applied on all model levels up to the top of the reanalysis data at 1 hPa. With the goal of the nudging being to constrain the model synoptic and larger-scale features, the nudging is applied in spectral space and is only applied up to total wave number 21. The reanalysis data are available with 6 h temporal resolution, and linear interpolation is used to derive fields at intermediate times. The application of nudging on only the large scales and the use of a relaxation time constant of 24 h have been found to produce root-mean-square differences between the nudged model and the reanalysis comparable to that found between different reanalysis data sets for fields such as temperature and vorticity [*Merryfield et al*., 2012].

Monthly average sea-surface temperatures and sea ice were specified from the Hadley Centre Global Sea Ice and Sea Surface Temperature data set [*Rayner et al*., 2003]. Time-varying lower boundary conditions for long-lived greenhouse gases (including CH_4 and N_2O) and ozone depleting substances were provided as an imposed mixing ratio in the lowest model layer following the Special Report on Emissions Scenarios A1b [*Intergovernmental Panel on Climate Change*, 2001] and A1 [*World Meteorological Organization*, 2011], respectively. The halocarbons are normally grouped into families in CMAM to reduce computational load, but for the runs used in this study, several trace gases, such as CFC-11 and CFC-12, were included as separate species that underwent photolysis but did not interfere with the ozone chemistry (F. Kolonjari, personal communication).

The measurements used in this work come primarily from the Atmospheric Chemistry Experiment Fourier Transform Spectrometer (ACE-FTS) instrument on the SCISAT satellite. ACE-FTS is a solar occultation instrument that has provided trace gas measurements since 2004 [*Bernath et al*., 2005]. ACE-FTS was designed primarily to measure the polar latitudes but does provide global coverage within three months. In this study we used level 2, version 3.0 CFC-11 and CFC-12 data averaged from June 2004 to May 2010 [*Boone et al*., 2013]. The mean age we used was derived from balloon in situ measurements of SF_6 and CO_2 and the TLP model as described in *Ray et al*. [2014].

3. The Modified Tropical Leaky Pipe Model

The original TLP model consists of a set of three coupled 1-D equations in the stratosphere, one for the tropics and one each for the southern and northern extratropics [*Plumb*, 1996; *Neu and Plumb*, 1999; *Hall*, 2000; *Hall and Waugh*, 2000]. The model includes advection, vertical diffusion, and horizontal mixing between the extratropics and tropics. We have used the TLP model as a starting point and modified it in order to study various aspects of the stratospheric transport. The main differences between the TLP model runs done here and in previous studies are the use of (1) common pressure altitude coordinates in all regions and (2) particle trajectories with photochemistry. These changes were done to facilitate comparisons between output from the TLP model and output from other models and measurements. In the original formulation of the TLP model [*Plumb*, 1996; *Neu and Plumb*, 1999] each latitudinal region used a separate equivalent height coordinate that was also unique to each trace gas. This simplified the model equations and allowed analytical solutions to be found for steady state conditions. Although this formulation is useful for theoretical exploration of steady state tracer distributions, it is not as useful for quantitative comparisons to trace gas profile measurements or global model output.

In the modified TLP model we use a Lagrangian formulation with realistic time varying inputs of the stratospheric residual mean circulation and mixing. This is a useful method of running the model to compare to measurements since the temporal variability of the stratospheric transport from the previous several years or more leaves an imprint on the measurements. This imprint is clearly seen in age spectra, which is the distribution of age of air within an air parcel at any location, which were shown to contain seasonal, quasi-biennial, and interannual modes of variability [*Ray et al*., 2014]. This formulation of the model can also be easily compared to global model output averaged over each of the latitudinal regions represented by the TLP model.

The relationship between mean circulation and mixing is constrained in each run by the vertically average mixing efficiency. The mixing efficiency is defined as $\overline{\varepsilon} = \alpha/\overline{\lambda}\overline{\tau}$ where $\overline{\lambda}$ is the mass flux out of the tropics due to the mean circulation and $\overline{\tau}$ is the time scale for the mass flux between the extratropics and tropics due to mixing [*Ray et al*., 2014; *Garny et al*., 2014a].

The expression for the mixing efficiency is inversely proportional to both the mixing time (τ) and the rate of mean circulation influence (λ). Thus, for example, if the mean circulation was to speed up causing λ to increase, while the mixing time remained the same, the mixing efficiencies would decrease. However, if we were to assume that the mixing efficiencies were constant then a speed up of the mean circulation would require the mixing times to decrease enough to counteract the increase in λ. In the TLP model runs performed in this study and in *Ray et al*. [2014] we used different values of $\overline{\varepsilon}$ to vary the mixing times for a particular residual mean circulation.

Vertical diffusion in the model is based on the Lagrangian trajectory diffusion technique in *Legras et al*. [2003]. The vertical motion due to diffusion is determined by the expression $d\eta = r\sqrt{2K_z dt}$ where K_z is the vertical diffusivity, dt is the time step of the model, and r is a random number uniformly distributed over $\left[-\sqrt{3}, \sqrt{3}\right]$. Based on estimates from previous observational studies [e.g., *Sparling et al*., 1997; *Legras et al*., 2003] and to be consistent with CMAM we used a value of $K_z = 0.01$ m^2/s in the tropics and 0.1 m^2/s in the extratropics.

The temporally and vertically varying inputs to the model are the mean meridional circulation and the mixing time scale between the extratropics and tropics. For the TLP model to conserve mass in each region the vertical velocities must satisfy the expression

$$\overline{w}^*{}_N(z,t) + \overline{w}^*_S(z,t) = -2\alpha\overline{w}^*_T(z,t). \quad (1)$$

Before the model was run this condition was tested on the input vertical velocities at each altitude and time step and if necessary the extratropical vertical velocites were adjusted by an equal amount in each hemisphere. Each model run was 25 years long to allow sufficient spin up time and had a time step of 4.5 days. The input vertical velocities and mixing times were interpolated from monthly means to the model time step.

For the TLP model runs performed here, the tropical boundaries are 22°N and 22°S and the extratropical regions extend to the poles, which means $\alpha = 0.6$. We chose these tropical boundaries because observational based estimates of the mean meridional circulation show that equatorward of these latitudes exists a region of persistent upwelling. The model was run with a vertical resolution of 200 m and a top altitude of 40 km above the tropopause. Each time step we released 1×10^4 particles at the tropical tropopause so that the total number of particles in the model at any one time following the spin up period was 2×10^5–5×10^5. Each particle was tagged with an initialization time as well as normalized CFC-11 and CFC-12 mixing ratios. The initialization time tag on the particles allowed the calculation of age of air using the lag time technique [e.g., *Waugh and Hall*, 2002]. The normalized CFC-11 and CFC-12 values were set to one at the tropical tropopause and at each time step, and for each particle a Bernoulli process was performed based on the local photochemical lifetime of each trace gas to determine if the gas was photochemically destroyed. Photolysis rates for CFC-11 and CFC-12 were from a 2-D stratospheric model and averaged over each latitudinal region in the TLP model [*Portmann et al*., 1999].

4. TLP Model Comparison to CMAM

An important test of the TLP model is how well it can reproduce output from a global CCM. If the TLP model is to be used as a diagnostic tool and intermediary between measurements and global models we need to

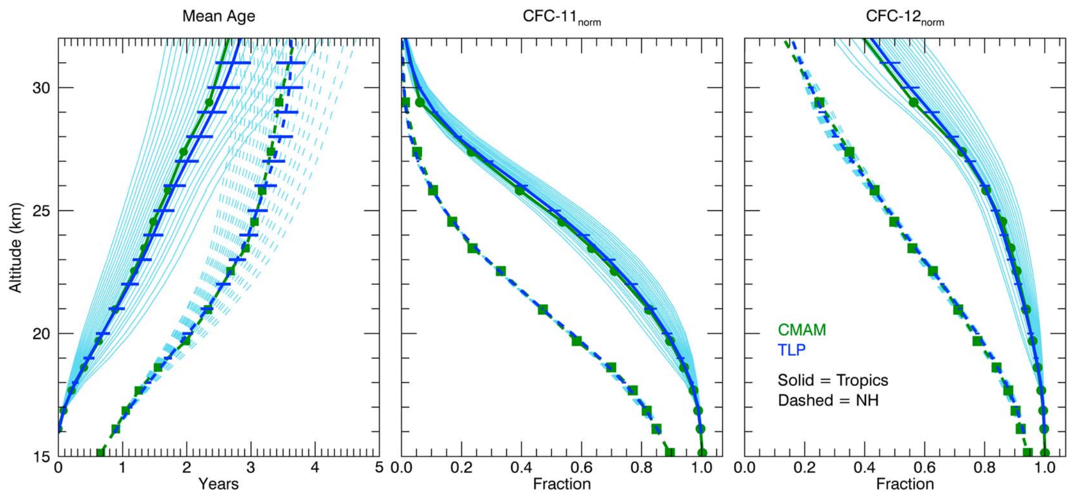

Figure 1. Average profiles of mean age, CFC-11, and CFC-12 from CMAM (green) and the TLP model (blue). Averages were taken from 2004 to 2010, and the solid lines with circle symbols represent the tropics, while the dashed lines with square symbols represent the Northern Hemisphere extratropics. The best fit of the TLP model output to CMAM output is shown by the dark blue lines, and the range of TLP model runs with mixing efficiencies from 0.16 to 1.6 is shown by the light blue lines. CFC-11 and CFC-12 were normalized to one at the tropical tropopause. CMAM tropical and midlatitude averages were taken over latitude ranges based on the modeled edges of the Tropical Pipe (see text for details).

establish that it accurately simulates global model output given the mean circulation as an input. The stratospheric mean circulation is a standard product output from global CCMs, and it was available from the CMAM run described in section 2 so this was used as input in the TLP model. However, the other input to the TLP model, the mixing time scale between the tropics and extratropics, is not a standard output. Thus, we can run the TLP model with the exact mean circulation from the CMAM run but then need to derive the mixing times to obtain the best fit to the CMAM output.

To derive the CMAM mixing time profile with the TLP model we performed a number of suites of TLP model runs where each suite contained 30 runs with a range of mixing efficiencies from 0.16 to 1.20. The initial suite consisted of mixing time profiles that were constant with height. Subsequent suites of TLP model runs contained adjusted shapes of the vertical mixing time profile based on the best match at each level of CFC-11, CFC-12, and mean age output from the two models. An iteration of TLP model runs was necessary since mixing at any one level in the stratosphere effects all other levels, especially the mean age [e.g., *Ploeger et al*., 2015], so it is not possible to solve for the mixing time at each level independently. The mixing times at each altitude had an assigned sinusoidal seasonal cycle with amplitude and phase in each hemisphere similar to that shown in *Ploeger et al*. [2012] since that study used ERA-Interim meteorology to derive the seasonality of mixing into the tropics.

The results of the mixing time iteration and best match of TLP and CMAM output are shown in Figure 1 for mean age and normalized CFC-11 and CFC-12. The profiles are averages from 2004 to 2010 and include the tropical and NH extratropical regions (the SH region was included in the analysis but is not shown). The full suite of runs is shown (light blue lines) to reveal the sensitivity to mixing of each quantity in each region. The agreement of the TLP best run to the CMAM averages is very good in all regions and for all the quantities. The error bars on the TLP model output are based on model runs where the mean age agreed to within ±0.3 years and the normalized CFC-11 and CFC-12 to within ±0.03. The best mixing time profile derived from the TLP model is shown in Figure 2. This best profile corresponds to the TLP model output profiles shown in Figure 1. The uncertainties in the mixing times are shown separately for mean age, CFC-11, CFC-12, and the combination of mean age and the tracers. The uncertainties in the mixing times at each level are based on a set of sensitivity runs where the mixing times in a 1 km thick layer centered at each level were set within a range from 0.2 to 5.0 years. Each level and each mixing time within the range were run individually, and the effects on the agreement with each trace gas and mean age at all other levels were taken into account. By doing the sensitivity runs this way the nonlocal effects of mixing on each quantity were taken into account. The individual uncertainties show the altitude regions the output

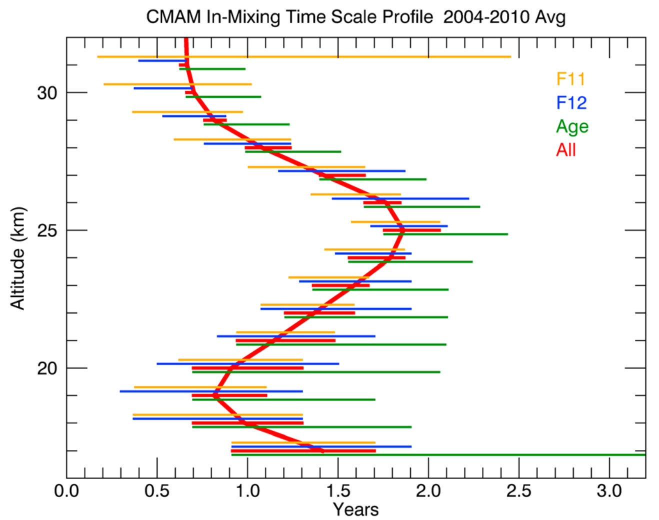

Figure 2. Profile of the average tropical in-mixing time in the CMAM model based on the best fits of CFC-11, CFC-12, and mean age from the TLP model. The uncertainty range for the trace gases was based on agreement within ±0.02 normalized mixing ratio between CMAM and TLP output. The uncertainty for mean age was based on agreement within ±0.25 years. The overall uncertainty on the best in-mixing profile (red lines) was based on the overlap in uncertainty for each tracer and mean age.

quantities are most sensitive to the mixing time. The uncertainties in the lowest part of the stratosphere are large since the tropical and extratropical values are similar there and mixing has a small effect. CFC-11 is most sensitive to mixing time variations from 20 to 26 km altitude as shown by the small uncertainties in this region, while CFC-12 has the smallest uncertainties above 25 km. Mean age is moderately sensitive to mixing throughout the stratosphere above 18 km.

An important aspect of this comparison between the TLP model and CMAM is to understand exactly how to average the CMAM output to best approximate the regions of the TLP model. As mentioned in the previous section the TLP model was run with tropical edges at 22°N and S. The tropical region between those latitudes represents the upwelling region of the stratosphere in the TLP model but we know that the actual region of upwelling in the stratosphere varies with altitude and with time [e.g., *Rosenlof*, 1995]. To account for this temporal latitude variability of the upwelling region in the mean circulation, we have averaged CMAM w* over the latitudes of strongest upwelling at each time and altitude within the range consistent with $\alpha = 0.6$ for input to the TLP model. If the region of strongest upwelling moved off the equator the latitudinal averaging region increased slightly to keep the area weighted averaging region the same as that centered over the equator. This averaging method allows the TLP model to best represent the total upward mass flux in the tropics and downward mass flux in the extratropics.

The CMAM trace gas and mean age output is averaged differently. After some experimentation the best fit was obtained by the use of tropical boundaries guided by the CMAM time-average turnaround latitudes, where the mean circulation changes from upwelling to downwelling. The turnaround latitudes are a function of altitude with the upwelling region narrowest in the lowest few kilometer of the stratosphere and wider with increasing altitude (not shown). The tropical boundary latitudes are set slightly equatorward of the time-average upwelling region so that the latitude range of each region closely satisfies $\alpha = 0.6$. From Figure 1 it is apparent that the tropical tracer profiles are sensitive to mixing but the extratropical tracer profiles are much less so due to the very small uncertainty in the NH tracer profiles (this will be discussed further in the next section). Thus, the agreement between the extratropical TLP and CMAM tracer profiles is largely determined by the extent of the extratropical latitude region the CMAM output is averaged over. The physical reason that it makes sense to average the trace gases and mean age over a constant in time latitudinal region is that the distributions of these quantities respond relatively slowly to the seasonal latitudinal variation of the strongest upwelling region. That is, the core of the tropics maintains its relative isolation from the extratropics even as the strongest upwelling region moves north and south of the equator. This analysis reveals that the TLP model can reasonably simulate the average extratropical region of a global model provided that the tropical boundaries are determined by the turnaround latitudes.

5. TLP Model Derived Mean Circulation and Mixing Based on ACE Measurements

With the TLP model established as an accurate approximation of the global CMAM output averaged in the tropical and extratropical regions we now use the TLP model as an intermediary between the global model and measurements. In Figure 3 normalized CFC-11, CFC-12, and mean age profiles averaged from 2004 to 2010 are shown for CMAM output and ACE satellite measurements. The measurement-based mean ages in

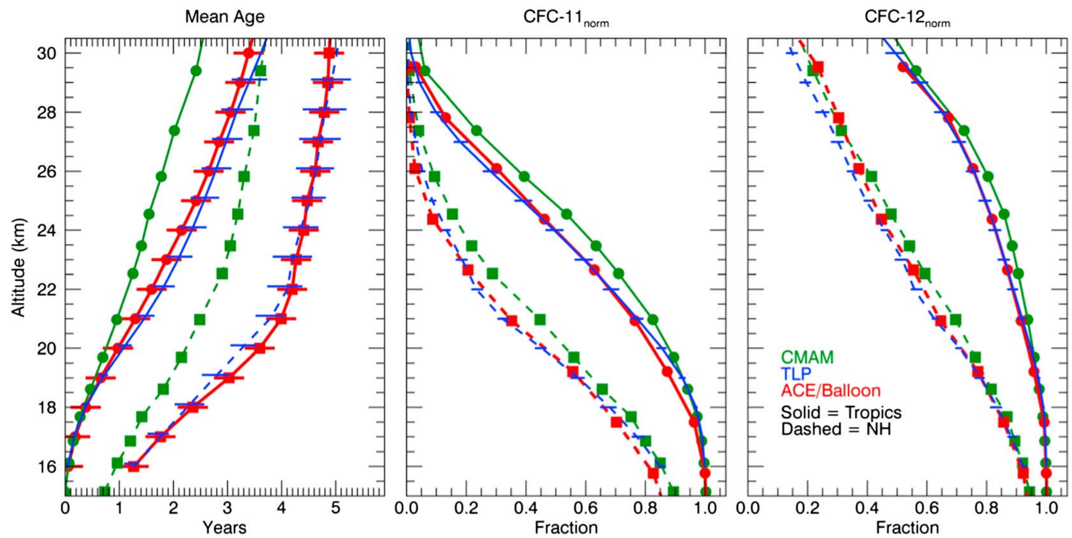

Figure 3. Average profiles over the time period 2004–2010 of (left) mean age, (middle) CFC-11, and (right) CFC-12 for CMAM output (green), measurements (red), and TLP output (blue). Measurement-based mean ages were calculated from in situ balloon profiles of SF_6 and CO_2 and the TLP model as in *Ray et al.* [2014]. CFC-11 and CFC-12 measurement profiles are from ACE. As in Figure 1, averages were taken from 2004 to 2010, and the solid lines with circle symbols represent the tropics, while the dashed lines with square symbols represent the Northern Hemisphere extratropics.

the NH are calculated from in situ balloon profiles of SF_6 and CO_2 and the TLP model as in *Ray et al*. [2014]. The tropical average mean age and SH profiles were calculated from the TLP model based on the mean circulation and mixing consistent with the NH mean ages.

The measurements and CMAM output disagree significantly throughout the stratosphere. The CMAM output has trace gas mixing ratios that are too large and mean age that is too young in both the tropics and extratropics. Each of the tracers and mean age are uniquely sensitive to mean circulation and mixing in the stratosphere as was indicated in the previous section (Figure 2) and is further quantified in this section. To diagnose possible reason(s) for the measured versus modeled discrepancies with only a global model would take considerable effort. Global models are expensive and time-consuming to run, but more importantly the wave activity that causes the stratospheric mean circulation and mixing has many varied sources and connections to other aspects of the modeled atmosphere. The breaking of planetary, synoptic, and gravity waves are tied to the basic state of the atmosphere but also help set the basic state. To make adjustments to model parameterizations or other model aspects to modify the wave breaking would alter much more than just the stratospheric mean circulation and mixing.

The TLP model can be used to diagnose unique mean circulation and mixing combinations necessary to accurately simulate the observed average profiles. As in the previous section we ran suites of TLP model runs that encompassed a range of different mean circulation strengths and mixing efficiencies. The initial suite of runs used the CMAM mean circulation and mixing times that were constant as a function of altitude but included seasonal variability. From that initial suite we adjusted the profile shapes based on the best match between modeled and measured CFC-11, CFC-12, and mean age at each level. We iterated over five suites of model runs to converge on mean circulation and mixing time profile shapes that would best match the measurements. We show results from the last suite of model runs that consisted of 19 different mean circulation strengths and 30 mixing efficiencies for each mean circulation, i.e., a total of 570 runs.

To evaluate how well each model run in the suite represented the measurements we averaged the absolute value of the model-measurement differences over an altitude range that spanned the middle and lower stratosphere and included both tropical and extratropical values. For extratropical CFC-11 we averaged from 16 to 27 km the altitude, while for CFC-12, mean age, and tropical CFC-11 we averaged from 16 to 29 km. The altitude and latitude ranges for averaging were chosen based on where measurements were available and, for CFC-11, where the mixing ratios were not close to zero. Also, for mean age the differences were taken from outside an uncertainty range of ±0.25 years around the measurement-based average value at each

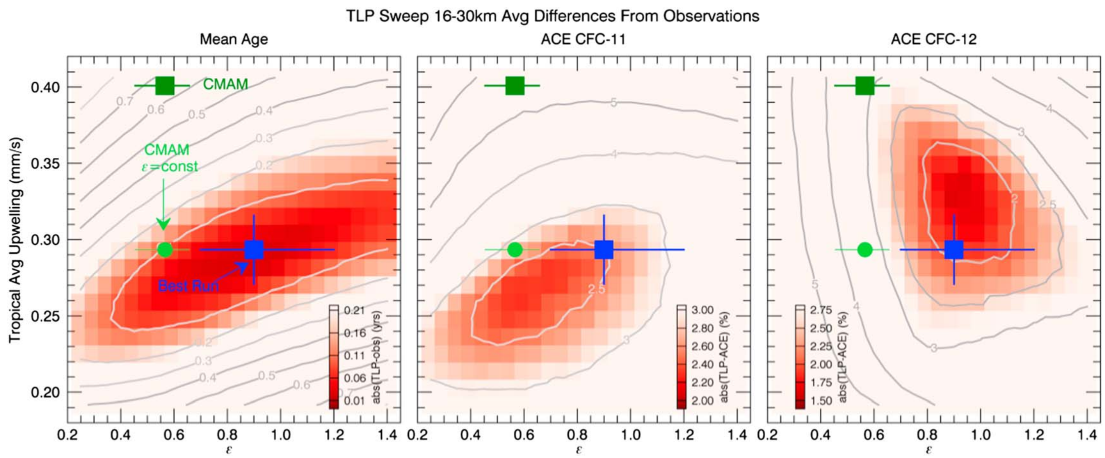

Figure 4. Results from TLP parameter sweep of tropical mean upwelling versus mixing efficiency (ε) averaged from 2004 to 2010. The tropical upwelling values represent averages over the 16–29 km altitude range. The red shaded squares represent individual TLP model runs with the darkness of the shading, indicating how well the TLP output matched ACE CFC-11 and CFC-12 measurements or measurement-based mean age. The TLP output and measurements were averaged in altitude from 16 to 29 km and over the tropics and NH. For the tracer differences the values are in percent, and for the mean age difference the values are in years. Contours of differences are also shown for values of 1.5, 2, 2.5, 3, and 4% for the tracers and 0.05, 0.1, 0.2, 0.4, and 0.6 years for mean age. The best run (blue square) had the lowest combined tracer and mean age differences. The CMAM average tropical upwelling and mixing efficiency is shown in green. The lime green circle indicates the results if the CMAM average tropical upwelling were decreased from the current value to the 0.25 mm/s value of the TLP best run while the CMAM mixing efficiency was kept constant at 0.33.

level, since we have insufficient measurements to determine single average mean age profiles in the tropics and NH.

The average absolute value of model-measurement differences for every model run of the suite are shown in Figure 4 as a function of mean tropical upwelling averaged from 16 to 29 km and the mixing efficiency (ε) averaged over the same altitudes. For the trace gases the best agreement, shown by the orange and red colors in Figure 4, is roughly 1.5–2.5%. The agreement with CFC-12 is on average better than that for CFC-11, as can also be seen in Figure 3. For mean age the average agreement is within 0.25 years for many different model runs.

The shape and slope of the region of best agreement are clearly different between mean age and each of the tracers. The region of best mean age agreement extends over a much larger range of ε, even past the edge of the plot toward higher ε. Whereas, each of the tracers has a much more confined region of agreement in ε. The reason for the different phase space covered by the regions of best agreement has to do with the different sources and sinks of the photolytic trace gases and mean age. Mean age is only dependent on the time an air mass has spent in the stratosphere, while photolytic trace gas mixing ratios are dependent on the path an air mass has taken and specifically, how much air has come from an altitude above which it is rapidly destroyed [e.g., *Hall*, 2000]. Thus, there are many combinations of upwelling and ε that result in the correct mean age since those quantities can effectively compensate each other to adjust both the tropical and extratropical values.

For the photolytic tracers, an interesting outcome of this work is that the effect of mixing on the extratropical average profiles was found to be strongly dependent on the altitude range over which the mixing occurred. Photolytic destruction of CFC-11 and CFC-12 is much more rapid in the tropics compared to the extratropics at any single altitude due to the increased solar radiation in the tropics. If most of the mixing occurred in altitudes below where the photolysis rapidly destroys one of the tracers then the average extratropical profile of that tracer was largely independent of mixing as shown in Figure 1. The mixing profile in Figure 2 shows that in CMAM the mixing times are fastest below roughly 22 km. The air that is mixed into the tropics at these altitudes will move upward, and subsequently, most of it will be transported back out to the extratropics by either the mean circulation or mixing within several kilometer of the original mixing event. This means that most of the air that is mixed into the tropics in the lower stratosphere is returned back to the extratropics without that air having experienced rapid photolysis and tracer loss that occurs only above certain levels in the tropics. So while each mixing event temporarily changes the extratropical and tropical tracer profiles, an average over many mixing events in the lower stratosphere will result in a very small change in the extratropical profile compared to that if no mixing had occurred. For the case of relatively fast mixing at altitudes greater than or equal to a level just below where rapid photolysis occurs in the tropics for a particular tracer then the extratropical profile of that tracer will be dependent on the amount of mixing. This is due to the fact that in this case the air moving from the extratropics to the tropics will experience significant additional loss of the photolytic tracer before being transported back to the extratropics.

The contrast in the regions of best agreement between the tracers and mean age in Figure 4 highlights the important point that each of these quantities contributes uniquely to constraining both the mean circulation and mixing. If only mean age is used to assess a model transport there are many different combinations of mean circulation and mixing that would result in a "successful" simulation, and likewise a mostly different set of combinations would successfully simulate CFC-11 and CFC-12. The use of both the tracers in combination with mean age provides much more information about the real stratospheric circulation and a more stringent test for models. Mean age and CFCs have been utilized to evaluate model transport in several previous studies [e.g., *Waugh et al*., 2007; *Douglass et al*., 2008], but the extensive ACE measurements, balloon measurement-based mean ages, and use of the TLP model in this study allow a much more detailed quantitative description of important aspects of the transport than has been done previously.

Based on the overlap in the regions of best agreement in Figure 4 a set of best tropical upwelling and mixing efficiency values can be identified (blue square and lines). The best values of tropical average upwelling range from 0.27 to 0.32 mm/s and the mixing efficiencies range from 0.7 to 1.2 with the single best agreement from a tropical upwelling of 0.29 mm/s and a mixing efficiency of 0.9. The TLP model output profiles from the best runs are shown in Figure 3 (blue lines) compared to the measurements (red lines) and CMAM output (green lines, same as in Figure 1). The agreement between the TLP output and the measured profiles is very good at nearly all levels and for all quantities in both the tropics and NH. Two exceptions are the tropical CFC-11 at 19 km where the TLP values are too high and the NH CFC-12 where the TLP output is too low. Overall, the uncertainties on the TLP best run values are smaller than the differences between CMAM output and the measurements at nearly all levels.

The mean tropical upwelling and mixing time profiles from the TLP best runs are shown in Figure 5 along with the corresponding CMAM profiles. The uncertainties on the CMAM mixing time profile are the same as the red lines in Figure 2. From these profiles and from Figure 4 it is clear that in order to better simulate the measurements the CMAM mean circulation needs to slow down at all levels, but most considerably below 22 km. From the mixing time profiles it is apparent that the CMAM mixing times need to increase to slow down the mixing below 25 km,. These are physically consistent changes since the mean circulation is driven by wave breaking, which also causes mixing between the tropics and extratropics. So a slower mean circulation would be expected to correspond to less mixing and longer mixing times. This is also consistent with the description in section 3 of the relationship between the mean circulation and mixing as defined by the mixing efficiency ε.

An interesting point to note is that ε was found by *Garny et al*. [2014a] to be essentially constant in the European Centre/Hamburg version 6 climate model across a range of mean circulation strengths from simulations of preindustrial time through the end of the 21st century. In follow-up work, *Garny et al*. [2014b] found that eight different climate models also conserved ε over different mean circulation strengths, although each climate model had a different ε that ranged from 0.3 to 1.2. The implication of this is if the CMAM average tropical upwelling strength was reduced from 0.4 to 0.29 mm/s as suggested by the TLP best run, while ε was conserved at the CMAM value of 0.55, then the mixing times would slow too much to match the measurements. The agreement with the tracers and mean age based on these circulation parameters can be seen in Figure 4 (lime green circles) to be improved over the original CMAM run in mean age and CFC-11 but not for CFC-12. To best match the tracers and mean age the CMAM mean circulation has to slow down and the mixing efficiency has to increase substantially from 0.55 to 0.9. The change in mixing efficiency is perhaps a more complicated requirement compared to the change in the mean circulation since the work of *Garny et al*. [2014a, 2014b] suggests that the mixing efficiency is an intrinsic aspect of each climate model.

The mean tropical upwelling values and in-mixing times derived here are largely consistent with previous estimates of these quantities. Quantitative comparisons with previous estimates are difficult due to the different latitudinal and temporal averaging among the studies. The tropical upwelling has been estimated

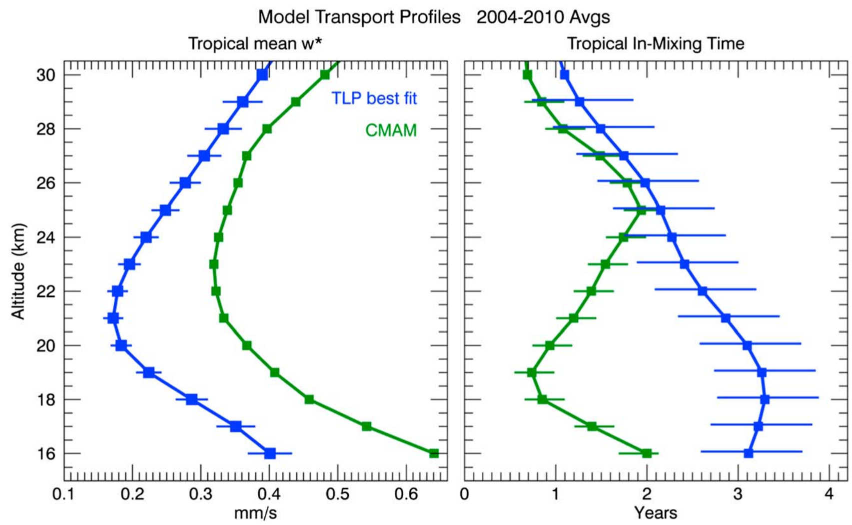

Figure 5. Profiles of average tropical mean upwelling and in-mixing times from CMAM (green) and the TLP model best fit to ACE tracer data and measurement based mean ages (blue). The lime green circles indicate the profiles if the CMAM tropical w* was adjusted to the TLP best run, while the CMAM mixing efficiency was kept constant at 0.33.

from many different techniques and data sets [e.g., *Rosenlof*, 1995; *Mote et al*., 1998; *Schoeberl et al*., 2008; *Abalos et al*., 2015; *Minschwaner et al*., 2015]. The recent study of *Abalos et al*. [2015] used three different reanalysis products and three different techniques to calculate the tropical upwelling and their average values between turnaround latitudes, and from 1979 to 2012, range from 0.25 to 0.55 mm/s at 16 km, 0.15 to 0.3 mm/s at 20 km, and 0.35 to 0.5 mm/s at 30 km. These are similar to the values found here although with a much larger spread among the estimates. Calculations of the tropical upwelling from the tape recorder signal of H_2O, or other tracers with seasonal variability, are slightly larger than the values found here [e.g., *Schoeberl et al*., 2008; *Minschwaner et al*., 2015] due to these studies use of data either at the equator or averages within 10–15° of the equator.

Previous estimates of in-mixing times have been derived from measurements and trajectories driven by reanalysis output [e.g., *Volk et al*., 1996; *Mote et al*., 1998; *Ploeger et al*., 2012]. As with the calculations of tropical upwelling, the methods and latitudinal and temporal averaging vary considerably among the studies. The recent study of *Ploeger et al*. [2012] used trajectories to derive average total in-mixing times of roughly 13 months in the 16–18 km layer of the tropical stratosphere. This corresponds to average in-mixing times of roughly 26 months from each of the SH and NH, which is somewhat shorter than the 30–40 month in-mixing times derived in this study.

The third input to the TLP model besides the residual circulation and mixing times is the vertical diffusion, which was held constant at values of 0.01 m^2/s in the tropics and 0.1 m^2/s in the extratropics. As mentioned in section 2 these values are consistent with previous studies and with the CMAM model. We tested other values of vertical diffusion in the extratropics ranging from 0 to 0.5 m^2/s (not shown). Results with values from 0 to 0.2 m^2/s were not considerably different than the results shown for a value of 0.1 m^2/s. But values of greater than 0.3 m^2/s resulted in output profiles that were unable to match the observed vertical gradients. To further constrain the vertical diffusion would require the use of a trace gas with a seasonal cycle in the lower stratosphere such as water vapor or CO_2.

6. Conclusions and Summary

The importance of the stratosphere in global chemistry-climate models brings along with it an increased importance in evaluating model performance in the stratosphere by comparisons with observations. The stratospheric circulation is driven by wave activity that propagates up from the troposphere so in order to adjust the stratospheric circulation in a CCM, important aspects of the tropospheric circulation and convection must be adjusted. Experimentation with a global CCM can be time-consuming, expensive, and not easily formulated.

An idealized model such as the modified TLP model described here can be effectively utilized to explore aspects of the stratospheric circulation that help explain measurement features. The TLP model only contains the stratosphere, and thus, changes to the stratospheric mean circulation and mixing can be prescribed easily so that many realizations can be performed. Over a thousand model runs were performed for the analysis described in this paper all on a personal desktop computer. The advantage of this kind of idealized modeling is that we can explore many possibilities and show unique aspects of the stratospheric circulation that best fit the measurements and the range of uncertainties on the circulation.

One key aspect of this work is the connection of the modified TLP model results to those from the global CCM CMAM. The analysis described in section 4 essentially ties the idealized model to the global model such that adjustments to the idealized model to fit stratospheric measurements should translate to the global model. There is still a complicated step to take from the TLP model stratospheric circulation that best matches the measurements to the tropospheric adjustments necessary in the global model to produce the ideal stratospheric circulation. In this case, the best run of the TLP model contained a slower mean circulation than CMAM (guided by ERA-Interim) at all levels and slower mixing times in the lowest part of the stratosphere below 24 km altitude.

The TLP model can act as an intermediary between measurements and global models but it is limited to providing quantitative guidance such as that described above, rather than a full solution. But that guidance is important information for the evaluation and progression of global CCMs. Global models are growing more complicated and so the need for idealized models to complement them is also growing. This study follows on previous efforts to evaluate stratospheric transport in CCMs [e.g., *SPARC CCMVal*, 2010], and there is clearly still more to be done to help guide specific improvements in the global models. In this work we focused on a specific time period (2004–2010) when ACE satellite measurements were available to compare to the CMAM output and we only compared time-averaged quantities. It is also possible to make more detailed comparisons of temporal variability on seasonal, QBO, and interannual time scales. This type of comparison would likely provide more useful information about how a global CCM should adjust to better match the measurements.

Another key aspect of this work is the quantification of the unique sensitivities of certain trace gases, CFC-11, and CFC-12, combined with the mean age of air, to the mean circulation and mixing between the tropics and extratropics. These sensitivities allowed a complete solution of the mean circulation and mixing combinations necessary to simultaneously simulate the trace gases and mean age. It is important to recognize trace gases such as these as priorities for future measurement programs [*Moore et al*., 2014] in order to continue to evaluate modeled stratospheric transport.

Acknowledgments
This work was supported by the NOAA Atmospheric Chemistry, Carbon Cycle, and Climate program. The CMAM simulations used for this work were made possible by financial support from the Canadian Space Agency through the CMAM20 project. More information and output from CMAM can be found at http://www.cccma.ec.gc.ca/. The Atmospheric Chemistry Experiment (ACE), also known as SCISAT, is a Canadian-led mission mainly supported by the Canadian Space Agency. ACE data can be accessed via the ACE-FTS website (registration required) http://www.ace.uwaterloo.ca.

References

Abalos, M., B. Legras, F. Ploeger, and W. J. Randel (2015), Evaluating the advective Brewer-Dobson circulation in three reanalyses for the period 1979–2012, *J. Geophys. Res. Atmos.*, *120*, 7534–7554, doi:10.1002/2015JD023182.

Bernath, P. F., et al. (2005), Atmospheric Chemistry Experiment (ACE): Mission overview, *Geophys Res Lett*, *32*, L15S01, doi:10.1029/2005GL022386.

Bertram, T. H., et al. (2007), Direct measurements of the convective recycling of the upper troposphere, *Science*, *315*, 816–820, doi:10.1126/science.1134548.

Boone, C. D., K. A. Walker, and P. F. Bernath (2013), Version 3 retrievals for the Atmospheric Chemistry Experiment Fourier Transform Spectrometer (ACE-FTS), in *The Atmospheric Chemistry Experiment ACE at 10: A Solar Occultation Anthology*, edited by P. F. Bernath, pp. 103–127 , A. Deepak, Hampton, VA.

Butchart, N., et al. (2011), Multimodel climate and variability of the stratosphere, *J. Geophys. Res.*, D05102, *116*, doi:10.1029/2010JD014995.

Dee, D. P., et al. (2011), The ERA-Interim reanalysis: Configuration and performance of the data assimilation system, *Q. J. R. Meteorol. Soc.*, *137*, 553–597, doi:10.1002/qj.828.

Douglass, A. R., R. S. Stolarski, M. R. Schoeberl, C. H. Jackman, M. L. Gupta, P. A. Newman, J. E. Nielsen, and E. L. Fleming (2008), Relationship of loss, mean age of air and the distribution of CFCs to stratospheric circulation and implications for atmospheric lifetimes, *J. Geophys. Res.*, *113*, D14309, doi:10.1029/2007JD009575.

Engel, A., et al. (2009), Age of stratospheric air unchanged within uncertainties over the past 30 years, *Nat. Geosci.*, *2*, doi:10.1038/ngeo388.

Garny, H., T. Birner, H. Bönisch, and F. Bunzel (2014a), The effects of mixing on age of air, *J. Geophys. Res. Atmos.*, *119*, 7015–7034, doi:10.1002/2013JD021417.

Garny, H., T. Birner, and H. Bönisch (2014b), The effects of mixing on stratospheric age of air in global models, *2014 EGU General Assembly*, Vienna, Austria.

Gerber, E. P., et al. (2012), Assessing and understanding the impact of stratospheric dynamics and variability on the Earth system, *Bull. Am. Meteorol. Soc.*, *93*, 845–859, doi:10.1175/BAMS-D-11-00145.1.

Hall, T. M. (2000), Path histories and timescales in stratospheric transport: Analysis of an idealized model, *J. Geophys. Res.*, *105*, 22,811–22,823, doi:10.1029/2000JD900329.

Hall, T. M., and D. W. Waugh (2000), Stratospheric residence time and its relationship to mean age, *J. Geophys. Res.*, *105*, 6773–6782, doi:10.1029/1999JD901096.

Intergovernmental Panel on Climate Change (2001), *IPCC Special Report on Emissions Scenarios: A Special Report of Working Group III of the Intergovernmental Panel on Climate Change*, Cambridge Univ., Press.

Kidston, J., A. A. Scaife, S. C. Hardiman, D. M. Mitchell, N. Butchart, M. P. Baldwin, and L. J. Gray (2015), Stratospheric influence on tropospheric jet streams, storm tracks and surface weather, *Nat. Geosci.*, *8*, 433–440, doi:10.1038/ngeo2424.

Legras, B., B. Joseph, and F. Lefevre (2003), Vertical diffusivity in the lower stratosphere from Lagrangian back-trajectory reconstructions of ozone profiles, *J. Geophys. Res.*, *108*(D18), 4562, doi:10.1029/2002JD003045.

Li, F., D. W. Waugh, A. R. Douglass, P. A. Newman, S. E. Strahan, J. Ma, J. E. Nielsen, and Q. Liang (2012), Long-term changes in stratospheric age spectra in the 21st century in the Goddard Earth Observing System Chemistry-Climate Model (GEOSCCM), *J. Geophys. Res.*, *117*, D20119, doi:10.1029/2012JD017905.

Manzini, E., et al. (2014), Northern winter climate change: Assessment of uncertainty in CMIP5 projections related to stratosphere-troposphere coupling, *J. Geophys. Res. Atmos.*, *119*, 7979–7998, doi:10.1002/2013JD021403.

McIntyre, M. E., and T. N. Palmer (1983), Breaking planetary waves in the stratosphere, *Nature*, *305*, 593–594.

McLandress, C., and T. G. Shepherd (2009), Simulated anthropogenic changes in the Brewer-Dobson circulation, including its extension to high latitudes, *J. Clim.*, *22*, 1516–1540, doi:10.1175/2008JCLI2679.1.

Merryfield, W. J., W.-S. Lee, G. J. Boer, V. V. Kharin, J. F. Scinocca, G. M. Flato, R. S. Ajayamohan, and J. C. Fyfe (2012), The Canadian Seasonal to Interannual Prediction System. Part I: Models and initialization, *Mon. Weather Rev.*, *141*, 2910–2945, doi:10.1175/MWR-D-12-00216.1.

Minschwaner, K., A. E. Dessler, J. W. Elkins, C. M. Volk, D. W. Fahey, M. Loewenstein, J. R. Podolske, A. E. Roche, and K. R. Chan (1996), Bulk properties of isentropics mixing into the tropics in the lower stratosphere, *J. Geophys. Res.*, *101*, 9433–9439, doi:10.1029/96JD00335.

Minschwaner, K., H. Su, and J. H. Jiang (2015), The upward branch of the Brewer-Dobson circulation quantified by tropical stratospheric water vapor and carbon monoxide measurements from the Aura Microwave Limb Sounder, *J. Geophys. Res. Atmos.*, *121*, 2790–2804, doi:10.1002/2015JD023961.

Moore, F. L., E. A. Ray, K. H. Rosenlof, J. W. Elkins, P. Tans, A. Karion, and C. Sweeney (2014), A cost effective trace gas measurement program for long term monitoring of the stratospheric circulation, *Bull. Am. Meteorol. Soc.*, doi:10.1175/BAMS-D-12-00153.1.

Mote, P. W., T. J. Dunkerton, M. E. McIntyre, E. A. Ray, P. H. Haynes, and J. M. Russell III (1998), Vertical velocity, vertical diffusion, and dilution by midlatitude air in the tropical lower stratosphere, *J. Geophys. Res.*, *103*, 8651–8666, doi:10.1029/98JD00203.

Neu, J. L., and R. A. Plumb (1999), Age of air in a “leaky pipe” model of stratospheric transport, *J. Geophys. Res.*, *104*, 19,243–19,255, doi:10.1029/1999JD900251.

Ploeger, F., P. Konopka, R. Müller, S. Fueglistaler, T. Schmidt, J. C. Manners, J.-U. Groob, G. Gunther, P. M. Forster, and M. Riese (2012), Horizontal transport affecting trace gas seasonality in the Tropical Tropopause Layer (TTL), *J. Geophys. Res.*, *117*, D09303, doi:10.1029/2011JD017267.

Ploeger, F., M. Abalos, T. Birner, P. Konopka, B. Legras, R. Müller, and M. Riese (2015), Quantifying the effects of mixing and residual circulation on trends of stratospheric mean age of air, *Geophys Res Lett.*, *42*, 2047–2054, doi:10.1002/2014GL062927.

Plumb, R. A. (1996), A “tropical pipe” model of stratospheric transport, *J. Geophys. Res.*, *101*, 3957–3972, doi:10.1029/95JD03002.

Portmann, R. W., S. Brown, T. Gierczak, R. Talukdar, J. B. Burkholder, and A. R. Ravishankara (1999), Role of nitrogen oxides in the stratosphere: A reevaluation based on laboratory studies, *Geophys Res Lett*, *26*, 2387–2390, doi:10.1029/1999GL900499.

Ray, E. A., et al. (2010), Evidence for changes in stratospheric transport and mixing over the past three decades based on multiple data sets and tropical leaky pipe analysis, *J. Geophys. Res.*, *115*, D21304, doi:10.1029/2010JD014206.

Ray, E. A., et al. (2014), Improving stratospheric transport trend analysis based on SF_6 and CO_2 measurements, *J. Geophys. Res. Atmos.*, *119*, 14,110–14,128, doi:10.1002/2014JD021802.

Rayner, N. A., D. E. Parker, E. B. Horton, C. K. Folland, L. V. Alexander, D. P. Rowell, E. C. Kent and A. Kaplan (2003), Global analyses of sea surface temperature, sea ice, and night marine air temperature since the late nineteenth century, *J. Geophys. Res.*, *108*(D14), 4407, doi:10.1029/2002JD002670.

Rosenlof, K. H. (1995), Seasonal cycle of the residual mean meridional circulation in the stratosphere, *J. Geophys. Res.*, *100*, 5173–5191, doi:10.1029/94JD03122.

Schoeberl, M. R., A. R. Douglass, B. Polansky, C. Boone, K. A. Walker, and P. Bernath (2005), Estimation of stratospheric age spectrum from chemical tracers, *J. Geophys. Res.*, *110*, D21303, doi:10.1029/2005JD006125.

Schoeberl, M. R., A. R. Douglass, R. S. Stolarski, S. Pawson, S. E. Strahan, and W. Read (2008), Comparison of lower stratospheric tropical mean vertical velocities, *J. Geophys. Res.*, *113*, D24109, doi:10.1029/2008JD010221.

Scinocca, J., N. A. McFarlane, M. Lazare, J. Li, and D. Plummer (2008), Technical Note: The CCCma third generation AGCM and its extension into the middle atmosphere, *Atmos. Chem. Phys.*, *8*, 7055–7074, doi:10.5194/acp-8-7055-2008.

Stratospheric Processes and their Role in Climate Chemistry-Climate Model Validation Activity (SPARC CCMVal) (2010), SPARC Report on the Evaluation of Chemistry-Climate Models, V. Eyring, T. G. Shepherd, D. W. Waugh (Eds.), SPARC Report No. 5, WCRP-132, WMO/TD-No 1526.

Sparling, L. C., J. A. Kettleborough, P. H. Haynes, M. E. McIntyre, J. E. Rosenfield, M. R. Schoeberl, and P. A. Newman (1997), Diabatic cross-isentropic dispersion in the lower stratosphere, *J. Geophys. Res.*, *102*, 25,817–25,829.

Stolarski, R. S., D. W. Waugh, L. Wang, L. D. Oman, A. R. Douglass, and P. A. Newman (2014), Seasonal variation of ozone in the tropical lower stratosphere: Southern tropics are different from northern tropics, *J. Geophys. Res. Atmos.*, *119*, 6196–6206, doi:10.1002/2013JD021294.

Strahan, S. E., et al. (2011), Using transport diagnostics to understand chemistry climate model ozone simulations, *J. Geophys. Res.*, *116*, D17302, doi:10.1029/2010JD015360.

Volk, C. M., et al. (1996), Quantifying transport between the tropical and midlatitude lower stratosphere, *Science*, *272*, 1763–1768.

Waugh, D. W., and T. M. Hall (2002), Age of stratospheric air: Theory, observations and models, *Rev Geophys*, *40*(4), 1010, doi:10.1029/2000RG000101.

Waugh, D. W., S. E. Strahan, and P. A. Newman (2007), Sensitivity of stratospheric inorganic chlorine to differences in transport, *Atmos. Chem. Phys.*, *7*, 4935–4941.

World Meteorological Organization (2011), World Meteorological Organization Scientific Assessment of Ozone Depletion: 2010, Global Ozone Research and Monitoring Project–Report No. 52, Geneva, Switzerland.